The Journal of Immunology

Cutting Edge: NLRP12 Controls Dendritic and Myeloid Cell Migration To Affect Contact Hypersensitivity

Janelle C. Arthur, John D. Lich, Zhengmao Ye, Irving C. Allen, Denis Gris, Justin E. Wilson, Monika Schneider, Kelly E. Roney, Brian P. O'Connor, Chris B. Moore, Amy Morrison, Fayyaz S. Sutterwala, John Bertin, Beverly H. Koller, Zhi Liu and Jenny P-Y. Ting

J Immunol 2010; 185:4515-4519; Prepublished online 22 September 2010;
doi: 10.4049/jimmunol.1002227
http://www.jimmunol.org/content/185/8/4515

The Journal of Immunology is published twice each month by
The American Association of Immunologists, Inc.,
1451 Rockville Pike, Suite 650, Rockville, MD 20852

Print ISSN: 0022-1767 Online ISSN: 1550-6606.

Cutting Edge

THE JOURNAL OF IMMUNOLOGY

Cutting Edge: NLRP12 Controls Dendritic and Myeloid Cell Migration To Affect Contact Hypersensitivity

Janelle C. Arthur,[*,†] John D. Lich,[*,†] Zhengmao Ye,[†] Irving C. Allen,[†] Denis Gris,[†] Justin E. Wilson,[‡] Monika Schneider,[*,†] Kelly E. Roney,[*,†] Brian P. O'Connor,[†] Chris B. Moore,[†] Amy Morrison,[†] Fayyaz S. Sutterwala,[‡] John Bertin,[§] Beverly H. Koller,[¶] Zhi Liu,[*,‖] and Jenny P-Y. Ting[*,†]

Nucleotide-binding domain leucine-rich repeat (NLR) proteins are regulators of inflammation and immunity. Although first described 8 y ago, a physiologic role for NLRP12 has remained elusive until now. We find that murine *Nlrp12*, an NLR linked to atopic dermatitis and hereditary periodic fever in humans, is prominently expressed in dendritic cells (DCs) and neutrophils. *Nlrp12*-deficient mice exhibit attenuated inflammatory responses in two models of contact hypersensitivity that exhibit features of allergic dermatitis. This cannot be attributed to defective Ag processing/presentation, inflammasome activation, or measurable changes in other inflammatory cytokines. Rather, *Nlrp12*$^{-/-}$ DCs display a significantly reduced capacity to migrate to draining lymph nodes. Both DCs and neutrophils fail to respond to chemokines in vitro. These findings indicate that NLRP12 is important in maintaining neutrophils and peripheral DCs in a migration-competent state. *The Journal of Immunology*, **2010, 185: 4515–4519.**

Nucleotide-binding domain leucine-rich repeats (NLRs) constitute a large family of mammalian genes that are homologous to innate immune defense genes extending back to the plant kingdom. In animals, NLRs function as important components of inflammation and immunity. To date, at least five NLR proteins are predicted to form a large complex termed the inflammasome, which serves as a scaffold for caspase 1 activation and subsequent release of bioactive IL-1β and related cytokines. Other NLR proteins, such as NOD1, NOD2, and NLRX1, have been shown to function as regulators of inflammatory cytokines, chemokines, and antimicrobial peptides (1, 2); however, the in vivo functions of the majority of NLRPs remain to be elucidated.

We have previously shown that human *NLRP12* is expressed by monocytes/macrophages and granulocytes and inhibits the activation of noncanonical NF-κB by associating with and inducing proteasome-mediated degradation of NF-κB–inducing kinase (3, 4). More recently, mutations that result in a truncated form of NLRP12 are linked to hereditary periodic fevers that manifest with recurrent fevers, joint pain, and skin urticaria (5). In addition, a single nucleotide polymorphism in intron 9 of *NLRP12* is loosely associated with atopic dermatitis (6). In this study, we present, to our knowledge, the first identified in vivo role for NLRP12 by demonstrating its role in the migration of dendritic cells (DCs) and neutrophils. This impacts contact hypersensitivity (CHS), but cannot be attributed to impaired IL-1β production and hence is distinct from the inflammasome function.

Materials and Methods

Mice

Nlrp12$^{-/-}$ and *Nlrp3*$^{-/-}$ mice were generated by homologous recombination and backcrossed for nine generations to C57BL/6 (The Jackson Laboratory, Bar Harbor, ME) and maintained in specific pathogen-free housing. OT-II mice, which express the OVA 323–339-specific TCR transgene on the C57BL/6 background, were kindly provided by M. Croft (La Jolla Institute of Allergy and Immunology, La Jolla, CA). Experiments were performed with 6–12-wk-old age- and sex-matched mice in accordance with the National Institutes of Health *Guide for the Care and Use of Laboratory Animals* and the Institutional Animal Care and Use Committee guidelines of University of North Carolina at Chapel Hill (Chapel Hill, NC).

Nlrp12$^{-/-}$ *genotyping*

Genomic tail DNA was amplified with F1 5′-CCCACAAAGTGATGTTGGACTG-3′, F2 5′-GCAGCGCATCGCCTTCTATC-3′, and R1 5′-GAAGCAACCTCCGAATCAGAC-3′.

*Department of Microbiology and Immunology, †Lineberger Comprehensive Cancer Center, ¶Curriculum in Genetics and Molecular Biology, and ‖Department of Dermatology, University of North Carolina at Chapel Hill, Chapel Hill, NC 27599; ‡Inflammation Program, Department of Internal Medicine, University of Iowa, Iowa City, IA 52241; and §Pattern Recognition Receptor Discovery Performance Unit, Glaxo-SmithKline, Collegeville, PA 19426

Received for publication July 6, 2010. Accepted for publication August 17, 2010.

This work was supported by National Institutes of Health Grants A1063031, AI067798, DK38108, DE016326, and HL068141, a National Institutes of Health Research Service Trainee Award (to J.C.A., J.E.W.), and the American Cancer Society (to J.D.L.). J.P.-Y.T is a Sandler Program Awardee.

Address correspondence and reprint requests to Dr. Jenny P.-Y. Ting, University of North Carolina at Chapel Hill, School of Medicine, Campus Box 7295, Room 209, Chapel Hill, NC 27599. E-mail address: panyun@med.unc.edu

The online version of this article contains supplemental material.

Abbreviations used in this paper: BM, bone marrow; BMD, bone marrow-derived; BMDC, bone marrow-derived dendritic cell; CHS, contact hypersensitivity; cLPS, commercial LPS; DC, dendritic cell; iDCs, immatureDCs before maturation stimulus; LN, lymph node; mac, macrophage; mDCs, DCs after TNF-α maturation; MHC-II, MHC class II; NLR, nucleotide-binding domain leucine-rich repeat; no tx, no treatment; pIC, polyinosinic-polycytidylic acid; pLPS, phenol-purified LPS; UnTx, untreated; WT, wild-type.

www.jimmunol.org/cgi/doi/10.4049/jimmunol.1002227

Expression analysis of Nlrp12

cDNA was synthesized from total RNA using Moloney murine leukemia virus reverse transcriptase (Invitrogen, Carlsbad, CA). *Nlrp12* intron-spanning primers were: forward, 5′-GTCCAGACTCAGTCCACATA-3′, reverse 5′-GTATAAGGCCAGCTCGATCA-3′; and *GAPDH*: forward, 5′-TGAAGCAGGCATCTGAGGG-3′, reverse 5′-CGAAGGTGGAAGAGTGGGAG-3′. Cell populations were isolated as described: T cells and B cells by negative selection; neutrophils from bone marrow (BM) (7); DCs (8), macrophages (9), mast cells (10), and osteoclasts (11) from BM precursors; Raw264.7 macrophages from American Type Culture Collection (Manassas, VA); and resident peritoneal macrophages by lavage with PBS and overnight adherence.

Generation of DCs and isolation of neutrophils

DCs were generated from BM precursors as described (8). Neutrophils were purified from BM using a discontinuous Percoll (Sigma-Aldrich, St. Louis, MO) gradient as described (7). Purity was 80–90% by differential staining of cytospins and flow cytometry. Viability was >95%.

Contact hypersensitivity

Mice were sensitized by topical application of hapten to the footpads and depilated abdomen (12): either 200 μl 3% oxazolone (Sigma-Aldrich) in ethanol or 200 μl 0.5% FITC (Sigma-Aldrich) in 1:1 acetone/dibutyl phthalate (Sigma-Aldrich). Five days later, 20 μl 1% oxazolone in ethanol or 20 μl 0.5% FITC in acetone/dibutyl phthalate was topically applied to one ear. The opposite ear was mock-treated with solvent, and control mice were treated with solvent on both ears. After 24 h, mice were euthanized, and 8-mm circular samples of ear tissue were excised and weighed, then the weight of the carrier-treated ear was subtracted from that of the hapten-treated ear. Ear tissue was frozen on dry ice (see below) or fixed in formalin, paraffin embedded, sectioned, and stained with H&E. Immune cell infiltration was quantified as average pixel density ($\times 10^4$) using ImageJ software (National Institutes of Health, Bethesda, MD) from four fields per ear.

Ear tissue homogenates

Individual ears were manually homogenized in T-PER reagent (Thermo Fisher Scientific, Waltham, MA) using RNase/DNase-free plastic pestles (Kimble Kontes, Vineland, NJ) then sonicated. Total protein concentration was determined by Bradford assay (Bio-Rad, Hercules, CA). IL-1β, TNF-α, and myeloperoxidase (MPO) were measured by ELISA (IL-1β and TNF-α, BD Biosciences, San Jose, CA; MPO, Hycult Biotechnology, Uden, The Netherlands).

FITC-induced in vivo migration

Twenty microliters 0.5% FITC in 1:1 acetone/dibutyl phthalate was applied topically to both ears (13). After 24 or 48 h, draining (auricular and cervical) and nondraining lymph nodes (LNs) were removed. Cells were stained with fluorochrome-conjugated Abs: anti-CD11c (HL3, BD Biosciences), anti-CD19 (eBioscience, San Diego, CA), and anti-langerin/CD207 (eBioL31, eBioscience) and analyzed by flow cytometry using a CyAn ADP flow cytometer (Beckman Coulter, Fullerton, CA) and FlowJo software (Tree Star, Ashland, OR). Ear epidermal sheets (14) were stained with biotin-labeled anti–I-A^b (AF6-120.1, BD Biosciences) plus streptavidin-Alexa Fluor 595 (Invitrogen), then visualized by fluorescent microscopy. DCs per ×400 field are the mean of four fields per sample counted by a blinded reader.

OVA-induced in vivo migration

Mice were injected s.c. into one footpad with 20 μl Alexa Fluor 647-labeled OVA (2 mg/ml in PBS; Invitrogen) emulsified in CFA (15). After 24 h, draining (popliteal) and nondraining LNs were removed and analyzed by flow cytometry as above.

In vitro migration

BM-derived DCs (BMDCs) were seeded at 2×10^5 per upper well of 96-well transwell plates with 5-μm pores (ChemoTx System, NeuroProbe, Gaithersburg, MD), over chemokines (PeproTech, Rocky Hill, NJ) in serum-free RPMI and incubated at 37°C for 3 h. Migrated cells were quantified using XTT (Sigma-Aldrich). For neutrophil migration: 3-μm pores, cultured 40 min at 37°C, migrated cells quantified using ToxiLight Bioassay Kit (Lonza, Basel, Switzerland).

Statistics

Central tendencies are presented as mean ± SEM. Pairwise comparisons were made using two-tailed tests, all $\alpha = 0.05$: Mann–Whitney *U* test (in vivo, Figs. 1*B–E*, 3*B–D*); Student *t* test (in vitro, Figs. 2*F*, 2*G*, 4*I*); Wilcoxon matched-pairs (paired data, Fig. 3*E*); one-sample Wilcoxon signed-rank, hypothesized median 100% (Fig. 3*F*). Outliers were by Grubb's test and statistics computed with Prism 4 (GraphPad, San Diego, CA).

Results and Discussion

Nlrp12$^{-/-}$ mice were generated by replacing a region of exon 3 containing the Walker A and Walker B sequences with the neomycin resistance gene (Fig. 1*A*, 1*B*). *Nlrp12*$^{-/-}$ mice displayed no gross abnormalities, and there were no identifiable abnormalities in the cellularity of the peripheral blood, BM, spleen, or LNs (Supplemental Fig. 1). Similar to human *NLRP12*, murine *Nlrp12* was expressed in the BM and spleen and at the cellular level in neutrophils and DCs (Fig. 1*C*). Unlike human *NLRP12*, however, murine *Nlrp12* was not highly expressed in transformed Raw264.7 macrophages, macrophages differentiated from BM precursors, or macrophages resident within the peritoneum.

NLRP12 is not required for IL-1β secretion in response to TLR agonist including LPS + ATP stimulation

Given the critical role of other NLR proteins in IL-1β processing, we tested the ability of *Nlrp12*$^{-/-}$ cells to produce IL-1β poststimulation with a variety of elicitors. No significant difference in IL-1β production was detected in *Nlrp12*$^{-/-}$ versus wild-type (WT) BM cells or BMDCs stimulated with LPS, LPS + ATP, other TLR ligands, or TNF-α (Fig. 1*D*). As a positive control, *Nlrp3*$^{-/-}$ cells failed to produce IL-1β when properly stimulated (Fig. 1*D*). *Nlrp12* did not affect the production of IL-12p40, IL-6, and TNF-α (Supplemental Fig. 2*A–E*). In vivo, *Nlrp12*$^{-/-}$ mice treated with two doses of LPS trended toward reduced survival, but the difference was not statistically different, and there was no difference in liver and kidney function (Supplemental Fig. 2*F–H*). Thus, more

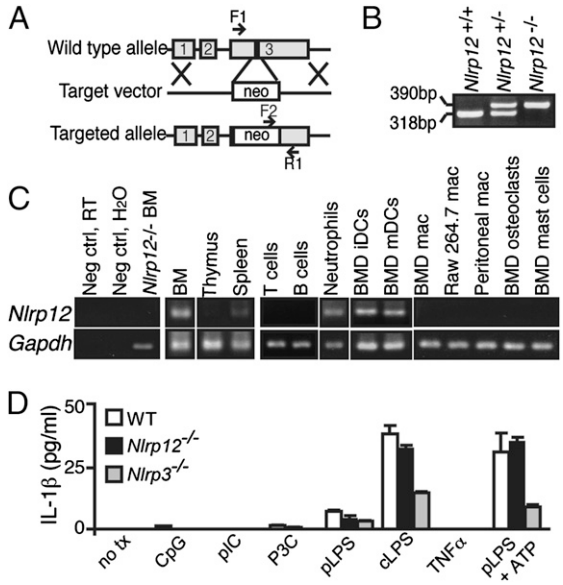

FIGURE 1. *A*, Targeted disruption of the *Nlrp12* gene. *B*, PCR genotyping from *Nlrp12*$^{+/-}$ crosses. *C*, Expression analysis of *Nlrp12* by RT-PCR. *D*, IL-1β production from BMDCs. BMD, BM-derived; cLPS, commercial LPS; iDCs, immature DCs before maturation stimulus; mac, macrophage; mDCs, DCs after TNF-α maturation; no tx, no treatment; pIC, polyinosinic-polycytidylic acid; pLPS, phenol-purified LPS.

extensive studies are required to delineate the role of *Nlrp12* in LPS-mediated inflammatory responses.

NLRP12 promotes hapten-induced CHS

The importance of *NLRP12* in cutaneous inflammation has been suggested through its recent linkage to human hereditary periodic fevers with skin urticaria (5). We evaluated the role of NLRP12 in cutaneous inflammation by assessing CHS, a mouse model of allergic dermatitis. WT and *Nlrp12*$^{-/-}$ mice were sensitized topically on the abdomen with hapten and either oxazolone or FITC and elicited 5 d later on the ear. Compared to controls, *Nlrp12*$^{-/-}$ mice displayed a weaker response to both haptens, as indicated by significantly reduced swelling (Fig. 2*A–C*) and reduced cellular accumulation at the site of elicitation (Fig. 2*D*). The partial effect of *Nlrp12* deletion is typical of other NLR responses in mice (16). During a CHS response, neutrophils migrate out of the bloodstream and into the affected skin tissue (17). In *Nlrp12*$^{-/-}$ mice, the accumulation of MPO-positive neutrophils in the skin was significantly reduced in hapten-treated ears compared with WT mice (Fig. 2*E*).

Others have shown that CHS is attenuated in *Nlrp3*$^{-/-}$ mice due to decreased IL-1β (18). Ear tissues from *Nlrp12*$^{-/-}$ mice did not show reduced IL-1β (Fig. 2*F*) or reduced TNF-α (Fig. 2*G*). These data suggest that *Nlrp12* does not affect inflammasome function or TNF-α in CHS.

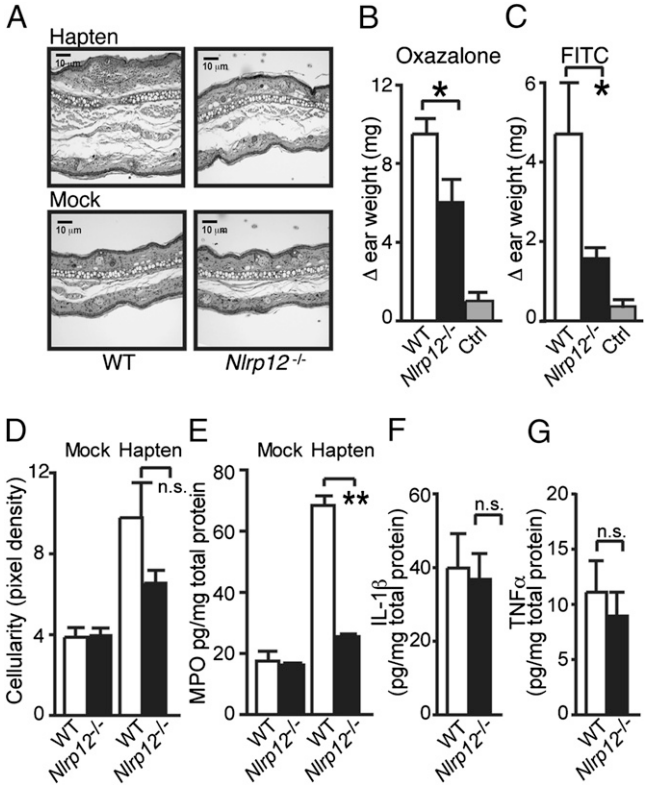

FIGURE 2. *Nlrp12*$^{-/-}$ mice fail to mount a robust CHS response. CHS-induced ear swelling in response to oxazalone (*A*, *B*; WT, $n = 12$; *Nlrp12*$^{-/-}$, $n = 13$; Ctrl, $n = 6$) and FITC (*C*; WT, $n = 7$; *Nlrp12*$^{-/-}$, $n = 8$; Ctrl, $n = 3$). *A*, H&E, original magnification ×40. *D*, Cellularity of CHS ear tissue (WT $n = 8$, *Nlrp12*$^{-/-}$, $n = 7$). *E*, Quantification of MPO$^+$ neutrophils in CHS ear tissue (WT, $n = 8$; *Nlrp12*$^{-/-}$, $n = 8$). IL-1β (*F*) and TNF-α (*G*) in CHS ear tissue (WT, $n = 5$; *Nlrp12*$^{-/-}$, $n = 5$). All experiments were repeated two to three times; all data are presented as mean ± SEM. $^*p < 0.05$; $^{**}p < 0.01$.

NLRP12 potentiates DC migration from the periphery to the draining LNs

Given the critical role of DCs in the CHS model (19) coupled with the high expression of *Nlrp12* in these cells, we determined if DC function is dependent upon NLRP12. Expression of MHC class II (MHC-II) and costimulatory factors CD80, CD86, and CD40 was not affected by *Nlrp12* during BMDC maturation (Supplemental Fig. 3*A–C*). To determine if *Nlrp12* affected Ag processing and presentation, WT and *Nlrp12*$^{-/-}$ BMDCs were pulsed with OVA and then cocultured with CFSE-labeled OT-II splenocytes specific for the OVA peptide 323–339. WT and *Nlrp12*$^{-/-}$ BMDCs induced equivalent Ag-dependent T cell proliferation, indicating that NLRP12 was not required for Ag presentation by DCs (Supplemental Fig. 3*D*, 3*E*).

A key function of DCs in the CHS model is to collect peripheral Ags and migrate to draining LNs. To evaluate DC migration in vivo, FITC was applied topically to the ears of WT and *Nlrp12*$^{-/-}$ mice. Draining LNs were removed 24 and 48 h later, and the presence of FITC$^+$ CD11c$^+$ DCs was assessed by flow cytometry. FITC$^+$ DCs in the draining LNs of *Nlrp12*$^{-/-}$ mice were significantly reduced compared with WT mice 24 and 48 h after FITC application (Fig. 3*A–C*). This was specific to *Nlrp12*$^{-/-}$ mice, as DC migration was comparable to WT in mice deficient in a related NLR, *Nlrp3*$^{-/-}$ (Fig. 3*D*). Migrated DCs in the draining LNs of WT mice were MHC-II$^+$ (mean ± SEM, 96.5 ± 0.86%) and immunostained for the dermal/epidermal DC marker langerin/CD207 (85.0 ± 2.30%). Similar results were obtained with *Nlrp12*$^{-/-}$ mice (MHC-II$^+$, 96.8 ± 0.65%; langerin/CD207$^+$, 88.1 ± 1.91%). In agreement with earlier results (Fig. 3*A–C*), the number of FITC$^+$ langerin/CD207$^+$ cells in the draining LNs of *Nlrp12*$^{-/-}$ mice was less than half that of WT mice (Fig. 3*E*), suggesting a defect in DC migration from the skin to the draining LNs. *Nlrp12*$^{-/-}$ DCs did not traffic to other immune organs, as FITC$^+$ CD11c$^+$ DCs were not detected in nondraining LNs, BM, or spleen (Fig. 3*A* and data not shown). Quantification of DCs in untreated skin revealed that *Nlrp12* did not affect DC numbers in untreated mice (Fig. 3*F*). However, following FITC treatment, the number of WT skin DCs decreased by >40%, whereas the number of *Nlrp12*$^{-/-}$ skin DCs changed by <10% (Fig. 3*F*), indicating that *Nlrp12* is required for DC egress from the skin.

To further examine the migratory capacity of *Nlrp12*$^{-/-}$ DCs, we measured migration of DCs to the draining LNs in response to s.c. OVA Ag. The absence of *Nlrp12* reduced OVA$^+$ DCs in the draining LNs by nearly 75% (Fig. 3*G*). These results support migratory defects in *Nlrp12*$^{-/-}$ DCs.

Nlrp12$^{-/-}$ *DCs and neutrophils fail to respond to chemokines in vitro*

DCs migrate to draining LNs in response to chemokine engagement of CCR7 and CXCR4 on DCs (20, 21). *Nlrp12* did not affect the expression of CCR7 and CXCR4 on BMDCs (Supplemental Table I). However *Nlrp12*$^{-/-}$ BMDCs demonstrated significantly reduced migration toward CCR7 and CXCR4 ligands CCL19, CCL21, and CXCL12 in an in vitro transwell assay (Fig. 4*A–C*, Supplemental Table II). In contrast, *Nlrp3*$^{-/-}$ BMDCs exhibited normal migration toward these chemokines (Fig. 4*D–F*). As a negative control, BMDCs from all genotypes failed to migrate toward CCL5 (Fig. 4*G*,

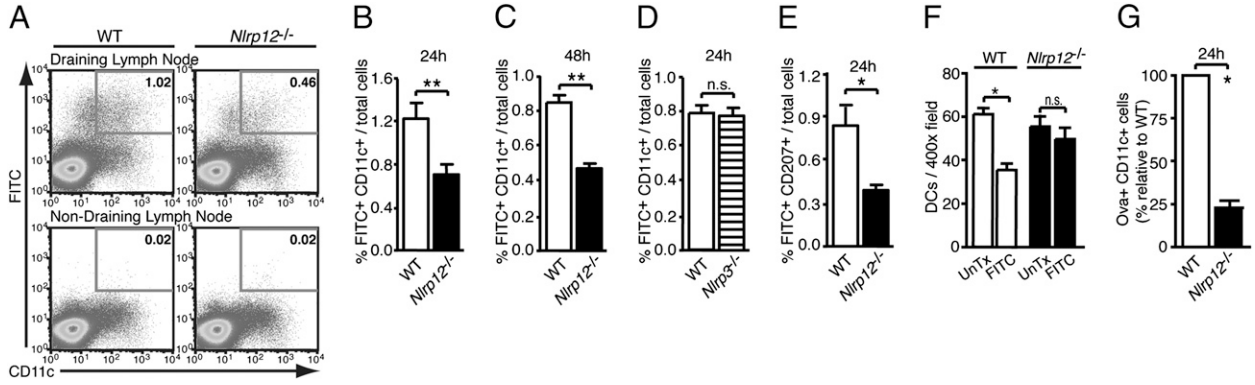

FIGURE 3. DC migration to draining LNs is significantly impaired in *Nlrp12*$^{-/-}$ mice. FITC$^+$ CD11c$^+$ cells in the draining LN 24 h (*A*, *B*) and 48 h (*C*) after topical application of FITC (WT, $n = 5$; *Nlrp12*$^{-/-}$, $n = 5$). *D*, FITC$^+$ CD11c$^+$ cells in the draining LN of WT ($n = 5$) and *Nlrp3*$^{-/-}$ ($n = 5$) after FITC. *E*, FITC$^+$ langerin/CD207$^+$ cells in the draining LN of WT ($n = 5$) and *Nlrp12*$^{-/-}$ ($n = 5$) mice after FITC. *F*, Quantification of I-Ab$^+$ skin DCs in ear epidermal sheets, untreated (UnTx) or FITC-treated (FITC) for 24 h (WT, $n = 4$; *Nlrp12*$^{-/-}$, $n = 5$). *G*, OVA$^+$ I-Ab$^+$ CD11c$^+$ cells in the draining LN 24 h following s.c. injection of fluorescent OVA in CFA. *Nlrp12*$^{-/-}$ values were normalized to WT values set at 100% (WT, $n = 6$; *Nlrp12*$^{-/-}$, $n = 5$). All experiments were repeated two to three times; all data are presented as mean ± SEM. $^*p < 0.05$; $^{**}p < 0.01$.

4*H*), a chemokine for immature DCs (22). The migration of *Nlrp12*$^{-/-}$ neutrophils to the neutrophil-attracting chemokine CXCL1 was also reduced by ~50% when compared with WT neutrophils (Fig. 4*I*).

NLR proteins intersect various pathways that are integral to inflammation and immunity (1). Based upon our previous observation of inappropriate noncanonical NF-κB activation

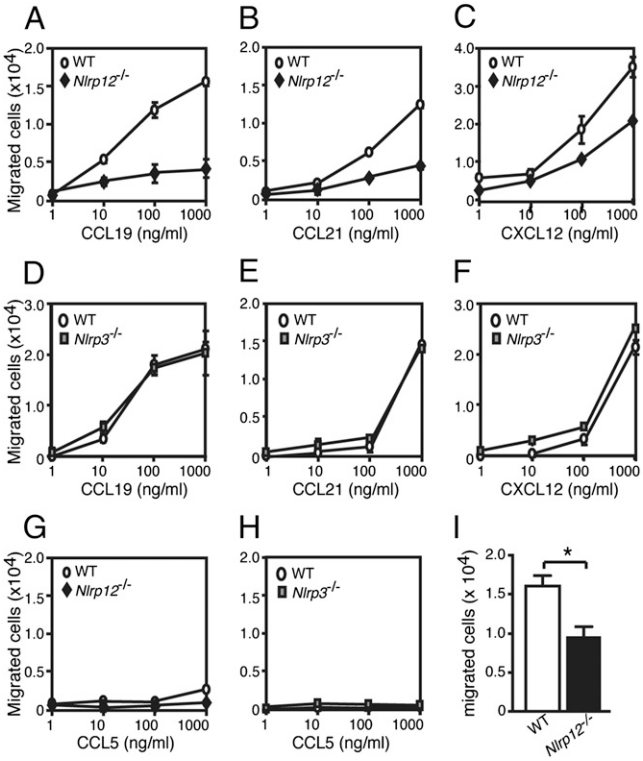

FIGURE 4. Deletion of *Nlrp12* impairs cell migration in vitro. Migration of WT (○) and *Nlrp12*$^{-/-}$ (♦) BMDCs (*A–C*, *G*) and WT (○) and *Nlrp3*$^{-/-}$ (■) BMDCs (*D–F*, *H*) to the indicated chemokine. Data are representative of three to five experiments and are presented as mean ± SEM of one experiment. Data from all experiments with associated pairwise comparison statistics are presented in Supplemental Table II. *I*, Migration of WT and *Nlrp12*$^{-/-}$ neutrophils to CXCL1. Data are comprised of three independent experiments, presented as mean ± SEM, and pairwise comparisons were made using two-tailed Student *t* test. α = 0.05. $^*p < 0.05$.

in human monocytic cell lines with reduced NLRP12, we predicted a proinflammatory phenotype for *Nlrp12*-deficient mice. Surprisingly, proinflammatory cytokine production was unaffected by the absence of NLRP12, and the CHS response mounted in these mice was significantly attenuated relative to WT mice. *Nlrp12* did not affect BMDC maturation or Ag-presenting functions in vitro. Instead, *Nlrp12* affected DC migration from the periphery to the draining LNs during CHS and s.c. immunization and migration to LN-homing chemokines. *Nlrp12* also affected neutrophil response to chemotactic stimuli, indicating a central role for NLRP12 in licensing cellular migration. Hereditary periodic fever is associated with two mutations in human *NLRP12* (5), and it is tantalizing to speculate that altered neutrophil migration or retention of activated DCs in the periphery may lead to the recurring cutaneous inflammation experienced by these patients. The current study does not address if DC progenitors can properly migrate from the BM to the skin in the absence of *Nlrp12*. Also, the mechanisms by which DCs and neutrophils rely on *Nlrp12* for optimal migratory capacity remain unclear.

We did not find an in vivo effect of NLRP12 on proinflammatory cytokine production. In contrast to these results, a previous study showed that silencing of *NLRP12* with small hairpin RNA leads to increased production of IL-6 and TNF-α in human cells of monocytic lineage (4). This implies that NLRP12 may exhibit distinct functions in DCs and monocytes/macrophages; however, because mouse macrophages do not express detectable *Nlrp12*, its deletion is not predicted to affect macrophage function in mice. Nonetheless, it will be interesting to investigate if the absence of *Nlrp12* affects monocyte egress from the BM to sites of inflammation. We also were unable to find an effect of *Nlrp12* deletion on IL-1β production, which is a well-established role for other NLRs. Human NLRP12 can colocalize with inflammasome components and promote IL-1β secretion when overexpressed (23). It is possible that the proper agonist/ligand, once identified, can activate NLRP12 inflammasome function. In agreement with previous studies from our group and others (4, 24), we found that NLRP12 was not required

for IL-1β secretion in response to TNF-α or TLR ligands ± ATP.

In summary, we reveal a regulatory role for NLRP12 in licensing cellular migration that affects a DC-dependent model of cutaneous inflammation. Unlike *Nlrp3*$^{-/-}$ mice, this is not correlated with a defect in inflammasome activation and IL-1β production. Considering that NLRs appear to cluster by their functional properties, it is likely that other NLRs will be found to similarly affect physiological processes by controlling cellular migration.

Disclosures

J.D.L. and J.B. are current employees and shareholders at GlaxoSmithKline. The other authors have no financial conflicts of interest.

References

1. Ting, J. P., J. A. Duncan, and Y. Lei. 2010. How the noninflammasome NLRs function in the innate immune system. *Science* 327: 286–290.
2. Kuenzel, S., A. Till, M. Winkler, R. Häsler, S. Lipinski, S. Jung, J. Grötzinger, H. Fickenscher, S. Schreiber, and P. Rosenstiel. 2010. The nucleotide-binding oligomerization domain-like receptor NLRC5 is involved in IFN-dependent antiviral immune responses. *J. Immunol.* 184: 1990–2000.
3. Lich, J. D., K. L. Williams, C. B. Moore, J. C. Arthur, B. K. Davis, D. J. Taxman, and J. P. Ting. 2007. Monarch-1 suppresses non-canonical NF-kappaB activation and p52-dependent chemokine expression in monocytes. *J. Immunol.* 178: 1256–1260.
4. Williams, K. L., J. D. Lich, J. A. Duncan, W. Reed, P. Rallabhandi, C. Moore, S. Kurtz, V. M. Coffield, M. A. Accavitti-Loper, L. Su, et al. 2005. The CATERPILLER protein monarch-1 is an antagonist of toll-like receptor-, tumor necrosis factor alpha-, and *Mycobacterium tuberculosis*-induced pro-inflammatory signals. *J. Biol. Chem.* 280: 39914–39924.
5. Jéru, I., P. Duquesnoy, T. Fernandes-Alnemri, E. Cochet, J. W. Yu, M. Lackmy-Port-Lis, E. Grimprel, J. Landman-Parker, V. Hentgen, S. Marlin, et al. 2008. Mutations in NALP12 cause hereditary periodic fever syndromes. *Proc. Natl. Acad. Sci. USA* 105: 1614–1619.
6. Macaluso, F., M. Nothnagel, Q. Parwez, E. Petrasch-Parwez, F. G. Bechara, J. T. Epplen, and S. Hoffjan. 2007. Polymorphisms in NACHT-LRR (NLR) genes in atopic dermatitis. *Exp. Dermatol.* 16: 692–698.
7. Boxio, R., C. Bossenmeyer-Pourié, N. Steinckwich, C. Dournon, and O. Nüsse. 2004. Mouse bone marrow contains large numbers of functionally competent neutrophils. *J. Leukoc. Biol.* 75: 604–611.
8. Wong, A. W., W. J. Brickey, D. J. Taxman, H. W. van Deventer, W. Reed, J. X. Gao, P. Zheng, Y. Liu, P. Li, J. S. Blum, et al. 2003. CIITA-regulated plexin-A1 affects T-cell-dendritic cell interactions. *Nat. Immunol.* 4: 891–898.
9. Johnson, C. R., D. Kitz, and J. R. Little. 1983. A method for the derivation and continuous propagation of cloned murine bone marrow macrophages. *J. Immunol. Methods* 65: 319–332.
10. Tertian, G., Y. P. Yung, D. Guy-Grand, and M. A. Moore. 1981. Long-term in vitro culture of murine mast cells. I. Description of a growth factor-dependent culture technique. *J. Immunol.* 127: 788–794.
11. Ruocco, M. G., S. Maeda, J. M. Park, T. Lawrence, L. C. Hsu, Y. Cao, G. Schett, E. F. Wagner, and M. Karin. 2005. IkappaB kinase (IKK)beta, but not IKKalpha, is a critical mediator of osteoclast survival and is required for inflammation-induced bone loss. *J. Exp. Med.* 201: 1677–1687.
12. Asherson, G. L., and W. Ptak. 1968. Contact and delayed hypersensitivity in the mouse. I. Active sensitization and passive transfer. *Immunology* 15: 405–416.
13. Thomas, W. R., A. J. Edwards, M. C. Watkins, and G. L. Asherson. 1980. Distribution of immunogenic cells after painting with the contact sensitizers fluorescein isothiocyanate and oxazolone. Different sensitizers form immunogenic complexes with different cell populations. *Immunology* 39: 21–27.
14. Sangaletti, S., L. Gioiosa, C. Guiducci, G. Rotta, M. Rescigno, A. Stoppacciaro, C. Chiodoni, and M. P. Colombo. 2005. Accelerated dendritic-cell migration and T-cell priming in SPARC-deficient mice. *J. Cell Sci.* 118: 3685–3694.
15. Itano, A. A., S. J. McSorley, R. L. Reinhardt, B. D. Ehst, E. Ingulli, A. Y. Rudensky, and M. K. Jenkins. 2003. Distinct dendritic cell populations sequentially present antigen to CD4 T cells and stimulate different aspects of cell-mediated immunity. *Immunity* 19: 47–57.
16. Muruve, D. A., V. Pétrilli, A. K. Zaiss, L. R. White, S. A. Clark, P. J. Ross, R. J. Parks, and J. Tschopp. 2008. The inflammasome recognizes cytosolic microbial and host DNA and triggers an innate immune response. *Nature* 452: 103–107.
17. Engeman, T., A. V. Gorbachev, D. D. Kish, and R. L. Fairchild. 2004. The intensity of neutrophil infiltration controls the number of antigen-primed CD8 T cells recruited into cutaneous antigen challenge sites. *J. Leukoc. Biol.* 76: 941–949.
18. Watanabe, H., O. Gaide, V. Pétrilli, F. Martinon, E. Contassot, S. Roques, J. A. Kummer, J. Tschopp, and L. E. French. 2007. Activation of the IL-1beta-processing inflammasome is involved in contact hypersensitivity. *J. Invest. Dermatol.* 127: 1956–1963.
19. Martin, S. F., and T. Jakob. 2008. From innate to adaptive immune responses in contact hypersensitivity. *Curr. Opin. Allergy Clin. Immunol.* 8: 289–293.
20. Kabashima, K., N. Shiraishi, K. Sugita, T. Mori, A. Onoue, M. Kobayashi, J. Sakabe, R. Yoshiki, H. Tamamura, N. Fujii, et al. 2007. CXCL12-CXCR4 engagement is required for migration of cutaneous dendritic cells. *Am. J. Pathol.* 171: 1249–1257.
21. Randolph, G. J., J. Ochando, and S. Partida-Sánchez. 2008. Migration of dendritic cell subsets and their precursors. *Annu. Rev. Immunol.* 26: 293–316.
22. Dieu, M. C., B. Vanbervliet, A. Vicari, J. M. Bridon, E. Oldham, S. Aït-Yahia, F. Brière, A. Zlotnik, S. Lebecque, and C. Caux. 1998. Selective recruitment of immature and mature dendritic cells by distinct chemokines expressed in different anatomic sites. *J. Exp. Med.* 188: 373–386.
23. Wang, L., G. A. Manji, J. M. Grenier, A. Al-Garawi, S. Merriam, J. M. Lora, B. J. Geddes, M. Briskin, P. S. DiStefano, and J. Bertin. 2002. PYPAF7, a novel PYRIN-containing Apaf1-like protein that regulates activation of NF-kappa B and caspase-1-dependent cytokine processing. *J. Biol. Chem.* 277: 29874–29880.
24. Meixenberger, K., F. Pache, J. Eitel, B. Schmeck, S. Hippenstiel, H. Slevogt, P. N'Guessan, M. Witzenrath, M. G. Netea, T. Chakraborty, et al. 2010. *Listeria monocytogenes*-infected human peripheral blood mononuclear cells produce IL-1beta, depending on listeriolysin O and NLRP3. *J. Immunol.* 184: 922–930.

Supplemental figure legends:

Fig. S1. Quantification of total cells in WT (○) or *Nlrp12*$^{-/-}$ (♦) (A), bone marrow (B), lymph nodes and (C), spleen. Total live cell number in bone marrow, spleen and lymph nodes were enumerated after red blood cell lysis using Trypan blue exclusion and hemacytometer. (D) Cellularity of peripheral blood.

Fig. S2. TLR stimulation (A), BMDCs were stimulated for 24 hours with the indicated agonists (Invivogen). No tx, unstimulated; P3C, TLR1/2 ligand Pam3Cys; HKLM, TLR2 ligand heat killed *Listeria monocytogenes;* pIC, TLR3 ligand polyinosinic:polycytidylic acid; St-FLA, TLR5 ligand flagellin from *Salmonella typhimurium;* FSL-1, TLR6/2 ligand; ssRNA, TLR7 ligand; ODN1826, TLR9 ligand. IL-12p40 was measured in supernatants by ELISA (BD Bioscience). (B-E), Freshly isolated bone marrow cells were stimulated with LPS or Pam3Cys (Invivogen) at the indicated concentrations. IL-6 and TNFα were measured in supernatants by ELISA (BD Bioscience). (F-H), LPS-induced endotoxic shock in *Nlrp12*$^{-/-}$ mice. Mice were injected i.p. with (F), 10 mg/kg or (G), 5 mg/kg of *E. coli* LPS (serotype 0111:B4; Invivogen). Mice were monitored for lethality twice daily for up to 14 days. Percent survival was compared between WT (○) and *Nlrp12*$^{-/-}$ (♦) mice and logrank test identified no significant differences between the groups. (H) Liver and kidney function in surviving mice from (B).

Fig. S3. Analysis of BMDC maturation and antigen presentation. BMDC from *Nlrp12*$^{-/-}$ and WT mice were collected on (A), days 8, (B),10, and (C), day 10 + 48hr TNFα and surface marker phenotype was determined by single-color flow cytometry after gating on live cells. The following PE-conjugated

antibodies were used: CD11c (N418; eBioscience), I-A^b (AF6-120.1; BD Biosciences), CD80 (53-6.7; BD Biosciences), CD86 (PO3.1; eBioscience), CD40 (1C10; eBioscience). Data are representative of three independent experiments. (D-E) Proliferation of OT-II splenocytes after co-culture with WT or *Nlrp12*$^{-/-}$ Ova-loaded DCs for (D) 3 days and (E) 5 days. BMDC from WT or *Nlrp12*$^{-/-}$ mice were pulsed with Ova whole protein (Worthington Biochemical Corp.) or mock-pulsed for 18-20 hours. Splenocytes were isolated from OT-II mice, labeled with CFSE (Invitrogen), and cultured 5:1 with BMDC (1×10^6) in 6-well plates. After 3-5 days in culture, cells were stained with biotin-labeled anti-Vβ5 (MR9-4 BD Biosciences), specific for the OTII transgenic TCR, followed by streptavidin-APC (eBioscience). Dilution of CFSE on Vβ5-positive cells was detected by flow cytometry.

Figure S1
Arthur, et al.

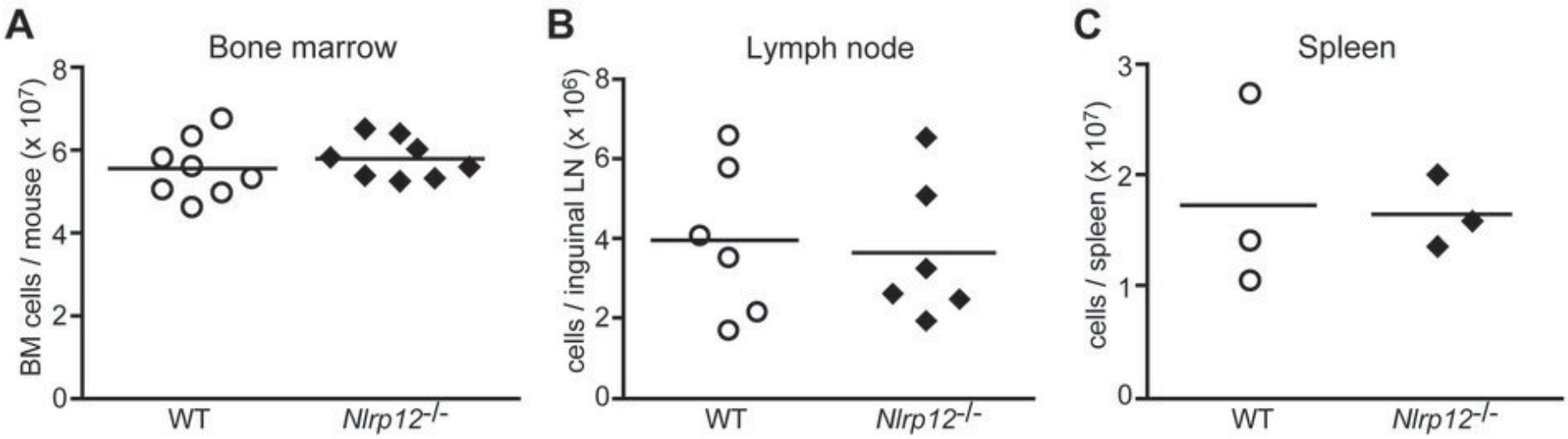

D

Cellularity of peripheral blood

	WBC (10^3/mm^3)	RBC (10^6/mm^3)	HGB (g/dl)	HCT (%)	MON (10^3/mm^3)	GRA (10^3/mm^3)	LYM (10^3/mm^3)
WT	8.5 ± 1.0	9.5 ± 0.2	15.3 ± 0.5	42.5 ± 1.4	0.8 ± 0.1	0.9 ± 0.0	6.8 ± 0.9
Nlrp12$^{-/-}$	7.2 ± 2.5	9.2 ± 0.4	14.5 ± 0.6	41.3 ± 1.7	0.7 ± 0.2	1.1 ± 0.3	5.4 ± 2.0

All values fall within normal reference ranges and depict mean ± s.e.m. WT n=3, *Nlrp12*$^{-/-}$ n=3.
WBC, white blood cells; HGB, hemoglobin; HCT, hematocrit; MON, monocytes; GRA, granulocytes; LYM, lymphocytes.
Mice were euthanized and cardiac blood was collected into tubes containing EDTA.
Analysis was performed by the Animal Clinical Chemistry and Gene Expression Laboratory at UNC Chapel Hill with the HESKA CBC Veterinary Hematology System.

Figure S2
Arthur, et al.

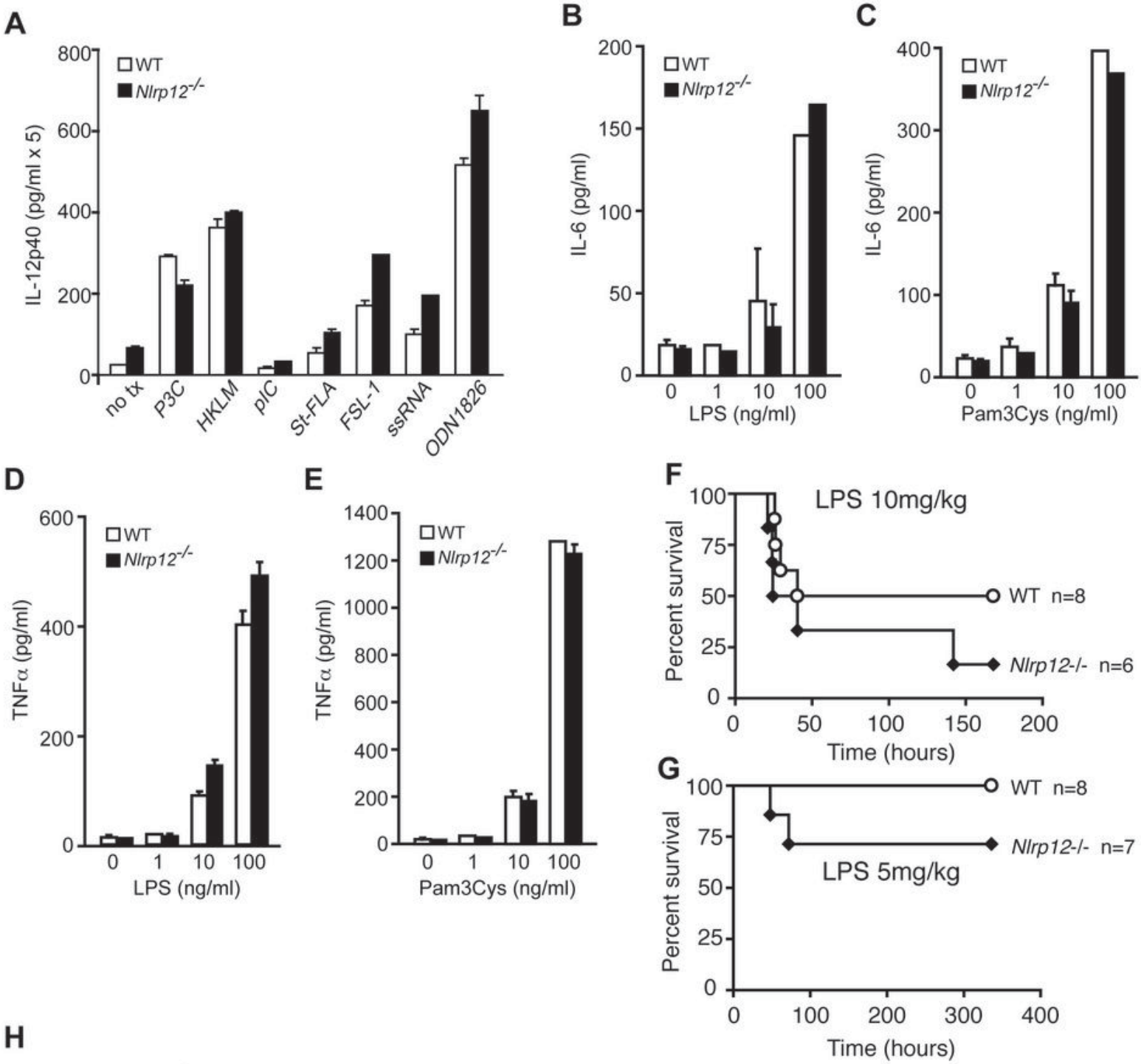

H

Liver and Kidney function

	Albumin (g/dL)	AST (U/L)	ALT (U/L)	ALP (U/L)	BUN (mg/dL)	Creatine (mg/dL)	Na+ (mmol/L)	Cl- (mmol/L)
WT	2.7± 0.2	69.4 ± 13.5	46.9 ± 1.6	32.1 ± 8.4	19.0 ± 0.9	0.1 ± 0.0	151.0 ± 1.9	114.8 ± 1.8
Nlrp12 $^{-/-}$	2.4 ± 0.2	71.4 ± 17.2	47.8 ± 0.9	35.2 ± 12.0	17.8 ± 1.6	0.1 ± 0.0	149.0 ± 1.4	120.4 ± 3.9

All values depict mean ± s.e.m. WT n=7, *Nlrp12* $^{-/-}$ n=5.
AST, aspartate aminotransferase; ALT, alanine aminotransferase; ALP, alkaline phosphatase; BUN, blood urea nitrogen.
Serum from survivors of the LPS endotoxic shock experiment (5 mg/kg) were tested for liver and kidney function
Analysis was performed by the Animal Clinical Chemistry and Gene Expression Laboratory at UNC Chapel Hill

Figure S3
Arthur, et al.

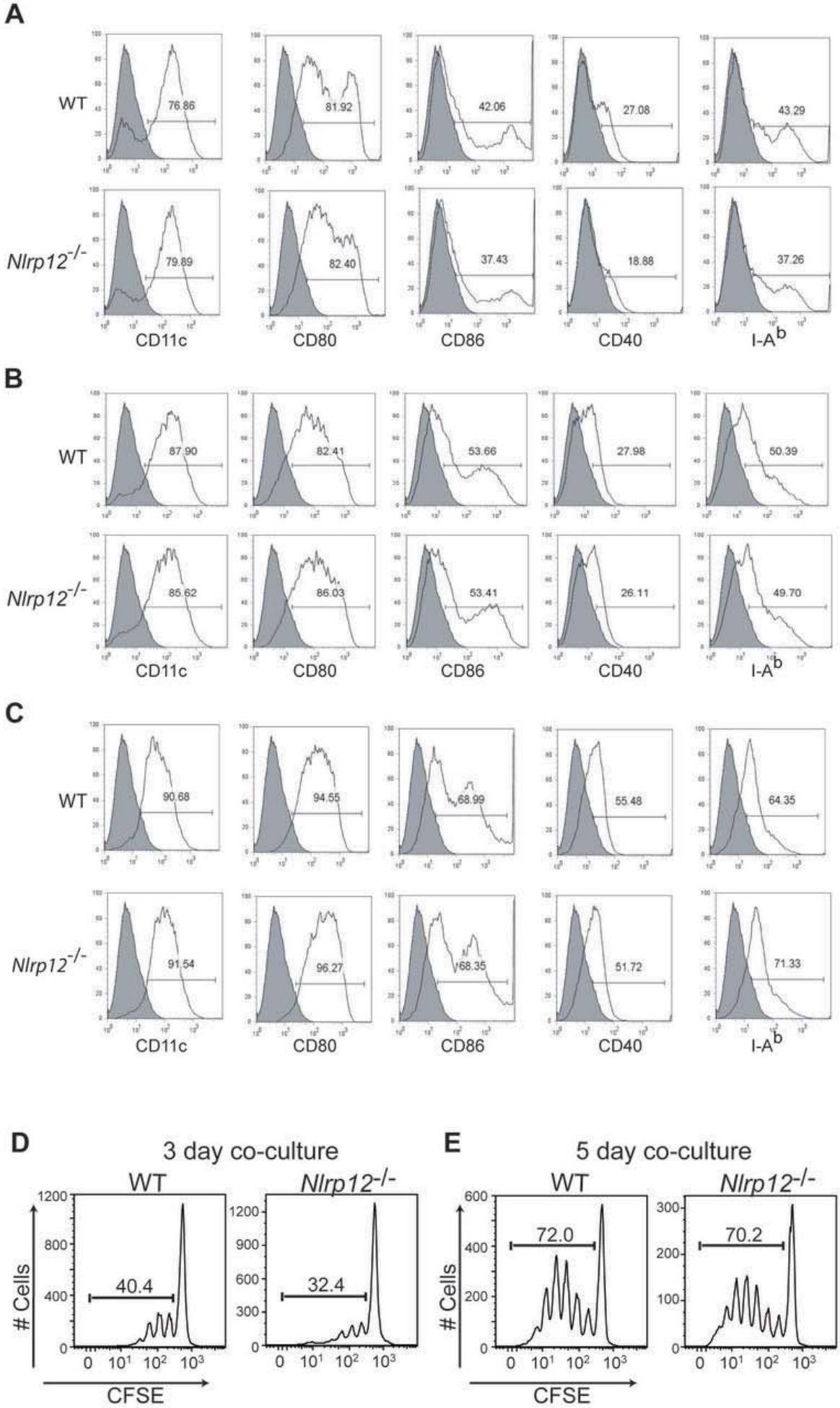

Table S1
Arthur, et al.

Table S1. Cell surface expression of CCR7 and CXCR4 on BMDC

BMDC days of differentiation:		day 8		day 10		day 10 + 48hr TNFα	
		% positive	MFI	% positive	MFI	% positive	MFI
CCR7	WT	27.0	143	24.6	195	37.9	354
	Nlrp12$^{-/-}$	24.9	136	24.3	192	40.0	308
CXCR4	WT	15.8	84	5.1	127	4.8	206
	Nlrp12$^{-/-}$	13.5	87	5.8	121	4.9	210

BMDC were differentiated with GM-CSF and IL-4 as described in Materials and Methods.
Cells were collected on the indicated days and stained with α-CD11c-PE-Cy7 (HL3, BD Biosciences), and either α-CCR7-APC (4B12, eBioscience) or α-CXCR4-AlexaFluor 647 (2B11, eBioscience).
Flow cytometry was used to evaluate CCR7 and CXCR4 expression on CD11c+ cells.
Data are from one experiment and representative of two independent experiments

Table S2
Arthur, et al.

Table S2. *In vitro* DC migration

Chemokine	Migrated cells		*n*	P value
CCL19 (ng/ml)	WT	*Nlrp12* -/-		
1000	19,813 ± 1,225	12,454 ± 1,082	5	0.0004 ***
100	16,527 ± 1,017	9,736 ± 982	5	0.0002 ***
10	6,569 ± 777	4,180 ± 416	5	0.0465 *
1	1,908 ± 520	2,120 ± 239	4	0.4025
CCL21 (ng/ml)				
1000	9,900 ± 1,633	3,814 ± 784	3	0.0244 *
100	2,941 ± 869	1,166 ± 404	3	0.1304
10	433 ± 194	352 ± 150	3	0.7962
1	272 ± 175	647 ± 309	3	0.6048
CXCL12 (ng/ml)				
1000	22,666 ± 2,527	15,530 ± 1,823	4	0.0338 *
100	14,270 ± 1,907	8,482 ± 1,568	3	0.0360 *
10	3,862 ± 841	2,766 ± 562	3	0.3865
1	1,127 ± 279	1,807 ± 298	2	0.2403
CCL5 (ng/ml)				
1000	915 ± 520	436 ± 174	3	0.8148
100	364 ± 152	553 ± 150	3	0.3213
10	420 ± 206	325 ± 153	3	0.7430
1	292 ± 119	916 ± 376	3	0.1996
Media				
	1,342 ± 324	1,071 ± 195	4	0.6446

Pairwise comparisons were made using a two-tailed Mann Whitney *U* test, $\alpha = 0.05$
The number of migrated cells is indicated as mean ± s.e.m.
XTT was used to calculate the number of migrated cells; the lowest standard was 1,563 cells.
The number of experiments are indicated as *n;* replicate wells were seeded in each experiment.